NASA CONTRACTOR REPORT

NASA CR-1074

NASA CR-1074

A LABORATORY SCALE MODEL TECHNIQUE FOR INVESTIGATING PNEUMATIC TIRE HYDROPLANING

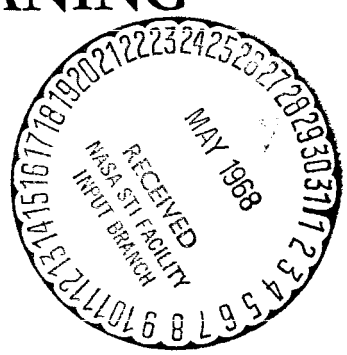

by H. Dugoff and I. R. Ehrlich

Prepared by
STEVENS INSTITUTE OF TECHNOLOGY
Hoboken, N. J.
for

NATIONAL AERONAUTICS AND SPACE ADMINISTRATION • WASHINGTON, D. C. • MAY 1968

NASA CR-1074

A LABORATORY SCALE MODEL TECHNIQUE FOR INVESTIGATING PNEUMATIC TIRE HYDROPLANING

By H. Dugoff and I. R. Ehrlich

Issued by Originator as Report No. 1223

Prepared under Contract No. NSR 31-003-016 by
STEVENS INSTITUTE OF TECHNOLOGY
Hoboken, N.J.

for

NATIONAL AERONAUTICS AND SPACE ADMINISTRATION

For sale by the Clearinghouse for Federal Scientific and Technical Information
Springfield, Virginia 22151 – CFSTI price $3.00

TABLE OF CONTENTS

	Page
SUMMARY	v
INTRODUCTION	vii
NOMENCLATURE	ix
ANALYSIS	1
TEST EQUIPMENT AND INSTRUMENTATION	5
Rolling Road	5
Water-Supply System	7
Tire Rig	8
Instrumentation	9
STATIC TESTS OF MODEL TIRES	11
Test Procedure	12
Test Results	13
Vertical-Force-Deflection Variations	13
Geometric Properties of Footprint Area	15
CONCLUDING REMARKS	17
REFERENCES	18
FIGURES (1 through 15)	19-29

SUMMARY

A new technique is developed for laboratory investigation of pneumatic-tire hydroplaning through experiment with small-scale tires on a treadmill runway-simulator. The tires are mounted on a modified aircraft-landing-gear assembly which permits freedom in heave under variable vertical load and allows measurement of the longitudinal force exerted on the tire. The treadmill is capable of speeds up to 90 feet per second, and is outfitted with a water-supply system and a nozzle which delivers a water layer 1-foot wide, of variable thickness, at matching speed.

The model tires are fabricated of polyurethane foam the density of which is varied to simulate variations in pneumatic-tire inflation pressure. Correlation of detailed load-deformation data for model and prototype tires demonstrates that geometric similarity is achieved under static conditions. Dimensional analysis has been employed to derive additional requirements for dynamic similarity and to develop a design for the initial series of experiments.

KEYWORDS

Hydroplaning
Tires
Scale Models

INTRODUCTION

It is by now a well-known fact that a pneumatic tire rolling or sliding over a water-covered surface may encounter a condition which results in its complete detachment from the surface; it then skis along on a film of water, a phenomenon known as hydroplaning. The hydroplaning of landing gear has been considered a causitive factor in a substantial number of aircraft runway accidents, and automotive engineers are beginning to recognize that even highway vehicles may be susceptible to hydroplaning at speeds well below legal limits.

Valuable experimental studies of the hydroplaning phenomenon have been carried out by personnel of the NASA Langley Research Center, on the full-scale hydroplaning test track and instrumented wheel fixture at that facility. These studies have led to the identification of many factors which affect hydroplaning and to the suggestion of various practical methods for its alleviation.[1,2] As of the present time, however, basic understanding of the hydroplaning phenomenon remains qualitative, intuitive, and essentially fragmentary.

One practical way to gain basic insight into the hydroplaning phenomenon would be through the conduct of a systematic experimental program in which the quantitative influence of each of the parameters reckoned to be of significance would be investigated. Such a program would naturally involve the conduct of a great many tests over a wide range of varying test conditions. For reasons of economics, the Langley test facility is clearly not suitable for such an exhaustive test program. It would appear, in fact, that any realistic technique for conducting such tests in full scale would involve prohibitive expense and, accordingly, that some model approach would be in order.

The Davidson Laboratory has previously performed scale-model simulations of pneumatic-tire performance in connection with various experimental studies of automotive-vehicle dynamics.[3,4] In one such application, the model tests were conducted on a treadmill "rolling road" facility.[5] The encouraging outcome of these tests suggested the possibility that a similar setup might profitably be utilized for scale-model hydroplaning studies. A hydroplaning

research program based on systematic rolling-road model tests was accordingly proposed to NASA, and its initial phases were implemented under NASA Contract DA 31003016. At the time this report was written, the development of the necessary test apparatus and procedures had been completed and actual testing was about to get underway. This interim report describes the test facilities and equipment, discusses the relevant scale-modeling theory in relation to the present program, and describes the development of small-scale tires fabricated of polyurethane foam, which are shown to possess static mechanical properties simulating full-scale pneumatic aircraft tires.

The authors would like to express their thanks to Messrs. S. A. Batterson, W. B. Horne, and U. T. Joyner of NASA Langley Research Center for their advice and cooperation throughout the course of this work. Important contributions by Messrs. D. M. Uygur, A. R. Schaefer, Jr., G. Wray, and I. O. Kamm of Davidson Laboratory, to the development of the experimental apparatus, the conduct of the static tire tests, and the preparation of this report, are also gratefully acknowledged.

NOMENCLATURE

A	gross tire footprint area
b	width of tire-ground contact area (footprint)
C_z	empirical coefficient related to tire vertical-force-deflection characteristics; see Eq. (15)
D	outside diameter of free tire
f	coefficient of friction between tire and adjacent surface
g	acceleration of gravity
H	horizontal force acting on tire
h	depth of undisturbed fluid on ground
ℓ	length of tire-ground contact area (footprint)
P	tire inflation pressure
P_{eq}	"equivalent total pressure" of polyurethane-foam tire; see Eq. (16)
P_r	rated pressure of tire
P_t	total pressure ($P + 0.08P_r$)
V	linear speed of tire
V_{cr}	hydroplaning inception speed
W	vertical force acting on tire
w	maximum width of undeflected tire
δ	vertical tire deflection
λ	geometrical scale factor; ratio between corresponding linear dimensions of model and prototype
μ	fluid viscosity
ρ	fluid density
σ	surface tension of fluid
ω	rotational speed of tire

Subscripts

$( )_m$	denotes quantities relating to model
$( )_p$	denotes quantities relating to prototype

Dimensionless Coefficients

$$\text{Froude number} = V/\sqrt{gh}$$

$$\text{Reynolds number} = \rho Vh/\mu$$

$$\text{Weber number} = \rho V^2 h/\sigma$$

ANALYSIS

There are two common systematic methods whereby modeling laws for a particular physical system may be derived.[6] The "equations approach" requires knowledge of the characteristic equations which govern the behavior of the system and therefore is manifestly not appropriate for the study of any phenomena involving the dynamics of pneumatic tires. The "parameters approach" requires only that the complete set of all variables affecting the system-behavior be specified. A variation of the second approach is employed here. Much of the difficulty associated with the description of tire dynamics is sidestepped for the moment by an assumption of geometrical similarity (including similarity of tire deformation). This assumption obviously is equivalent to the imposition of constraining relationships between certain parameters governing the dynamics of the model and prototype tires and, as will be seen subsequently, merely defers the problem of establishing the appropriate relationships to a later stage in the modeling process.

Below are the independent variables considered to affect the hydroplaning phenomenon:

D	Tire diameter*
h	Fluid depth
W	Tire load
V	Linear speed of tire
ω	Rotational speed of tire
μ	Fluid viscosity
ρ	Fluid density
σ	Surface tension of fluid
f	Coefficient of friction between tire and adjacent surface
g	Acceleration of gravity

*In view of the assumption of geometrical similarity, D represents the usual "characteristic linear dimension" of the tire.

The dependent variable presently considered is the horizontal force exerted on the tire by the ground, H. By application of conventional techniques of dimensional analysis,[7] the relation expressing its dependence upon the above independent variables may be obtained in the form

$$\frac{H}{W} = F\left(\frac{h}{D},\ f,\ \frac{V}{\omega D},\ \frac{\rho D^2 V^2}{W},\ \frac{V}{\sqrt{gh}},\ \frac{\rho V h}{\mu},\ \frac{\rho V^2 h}{\sigma}\right) \tag{1}$$

The model design conditions follow directly from Equation (1). Letting the subscript m denote quantities relating to the model, and the subscript p denote quantities relating to the prototype, sufficient conditions for the equality of H_m/W_m and H_p/W_p are

$$\frac{h_m}{D_m} = \frac{h_p}{D_p} \tag{2}$$

$$f_m = f_p \tag{3}$$

$$\frac{V_m}{\omega_m D_m} = \frac{V_p}{\omega_p D_p} \tag{4}$$

$$\frac{\rho_m D_m^2 V_m^2}{W_m} = \frac{\rho_p D_p^2 V_p^2}{W_p} \tag{5}$$

$$\frac{V_m}{\sqrt{g_m h_m}} = \frac{V_p}{\sqrt{g_p h_p}} \qquad \text{(Froude number)} \tag{6}$$

$$\frac{\rho_m V_m h_m}{\mu_m} = \frac{\rho_p V_p h_p}{\mu_p} \qquad \text{(Reynolds number)} \tag{7}$$

$$\frac{\rho_m V_m^2 h_m}{\sigma_m} = \frac{\rho_p V_p^2 h_p}{\sigma_p} \qquad \text{(Weber number)} \tag{8}$$

The conditions given by Equations (2) through (5) are easily met under a wide variety of test constraints. Equations (6) through (8), however, present a problem long familiar to scale-model experimenters in the field of hydrodynamics: the incompatibility of Froude-number $(\frac{V}{\sqrt{gh}})$, Reynolds-number $(\frac{\rho Vh}{\mu})$, and Weber-number $(\frac{\rho V^2 h}{\sigma})$ scaling. Because of this problem, it is not practically feasible to conduct a hydrodynamic model test without some measure of model distortion. Empirical methods of correcting for model distortion in conventional ship-model testing have been used by naval architects for many years,[8] and a systematic technique to account for its effects under more general conditions has been developed by Murphy.[7] For purposes of this study, it is first assumed that the influence of both viscosity and surface tension may be neglected, i.e., initial consideration is given to "dynamic hydroplaning."[1] An important aspect of the analysis of resulting experimental data is therefore the definition of the limits of applicability of this assumption in terms of both Reynolds number and Weber number.

Under the assumption of negligible viscous and surface-tension effects, the model design conditions are reduced to Equations (2) through (6), which can be simultaneously satisfied even under the convenient constraints

$$g_m = g_p \tag{9}$$

and

$$\rho_m = \rho_p \tag{10}$$

That is, the model can be tested with the same fluid as the prototype under the same gravitational conditions. Simultaneous solution of Equations (2) through (6), (9) and (10) results in the following set of simplified design conditions:

$$h_m = \lambda h_p \tag{11}$$

$$V_m = \sqrt{\lambda}\, V_p \tag{12}$$

$$\omega_m = \frac{1}{\sqrt{\lambda}}\, \omega_p \tag{13}$$

$$W_m = \lambda^3 W_p \tag{14}$$

$$f_m = f_p \text{ (Equation 3)}$$

where $\lambda = D_m/D_p$ is the geometrical scale ratio for the experiment.

TEST EQUIPMENT AND INSTRUMENTATION

Construction and instrumentation of the test apparatus comprised the major effort of this phase of the study. To conduct the required tests, it was necessary to provide a simulated runway surface, an adequate water supply, a rig on which to mount the test tires, and instrumentation to measure test conditions. Figure 1 is a photograph of the completed hydroplaning-model-test facility.

Rolling Road

To simulate the runway surface, an existing conveyor-belt apparatus called the "rolling road" was upgraded to have operating characteristics appropriate for hydroplaning testing. Figure 2 illustrates the basic principle of operation of the rolling road. The moving belt, 3 feet in width, is stretched over a parallel pair of 20-in.-OD hollow cylindrical drums. Power is supplied to the system through torque acting on one of these drums. Friction between the rubber-coated drum surface and the tightly stretched nylon belt causes the belt to move over the powered drum without slipping. More general information concerning the rolling road may be found in an earlier publication.[5]

For purposes of this study, the following modifications were made:

(a) Increased Power

The existing 5-hp drive motor was replaced by a 40-hp direct-current unit powered and controlled by the output from a closed-loop, 50-kw motor-generator set. The d-c generator is driven by a 440-v a-c motor. The d-c generator field is excited by a d-c amplifier of variable output, and the armatures of the generator and rolling-road drive motor are coupled. The field of the rolling-road drive motor is excited by a constant source. To maintain constant speed, there is a feedback which closes the loop between the drive motor and the d-c amplifier input.

The existing rubber "timing belt" power-transmission system was replaced by a heavier-duty system of the same type and the rolling-road drums were dynamically balanced for operation at higher rotative speeds.

The up-powered drive system is capable of providing rolling-road speeds in excess of 90 feet per second.

(b) Installation of a Translucent Belt

It was felt that pictures of the tire-road contact patch, taken from below, would be a valuable complement to the quantitative data obtained during the program. Investigation disclosed that belts of available transparent materials were not suitable for the present application, because of insufficient strength, particularly at the transverse seam. Oriented nylon, although not transparent, is translucent and permits reasonably clear pictures to be taken of objects within about one inch of the surface. This material was therefore considered acceptable from an optical standpoint. Stress tests demonstrated that it could be fabricated with the requisite strength properties.

The existing rubber-belt system was therefore replaced by a translucent, oriented nylon belt 0.060-in. thick, 36-in. wide, and 28-ft long. The extreme longitudinal stability of the oriented nylon caused the belt to buckle under the non-uniform tension applied by the crowned, steel idler pulley, but bands of thick rubber, mounted near the outside rims of the idler drum, eliminated this effect and have been generally successful in providing a level, flat test-surface.

Heat generated by friction between the nylon belt and the teflon-coated support table is low enough to be dissipated without recourse to lubrication or to the use of a secondary belting system as in the original rubber-belting setup.[5] Air entrainment between the belt and the teflon surface sometimes causes the belt to "hop" slightly. If this condition proves detrimental during future testing, grooves in the surface may be required for relief.

A plexiglass-mirror system to permit observation and photography of the tire footprint was designed but has not yet been constructed. Installation is being delayed pending completion of experiments to determine the optimum section of the rolling road for hydroplaning tests.

Water-Supply System

The water system installed to simulate wet and flooded runways (Figures 1, 3, 4, and 5) is designed to deposit on the rolling road a 12-in.-wide layer of water of variable thickness, flowing at a speed the same as the belt speed.

(a) Water-Circulation System

The water-circulation system consists of a centrifugal pump, capable of generating a 150-ft head, with an integral 25-hp, 100-v a-c power pack. It draws water from a reservoir with a capacity of $37\frac{1}{2}$ cubic feet, through 4-in. piping, and delivers it to the nozzle. A 3-in. bypass line from the outlet of the pump returns water to the reservoir. Water-flow rate is grossly controlled by adjusting gate valves which control the flow to the nozzle and through the bypass line. Maximum flow is obtained when the nozzle valve is fully open and the bypass valve is fully closed. A 1-in. line controlled by a gate valve, in parallel with the supply line, provides for fine adjustment of the flow. A totalizing type of flow meter is installed just ahead of the nozzle to measure the flow. Water discharged from the end of the rolling road is collected by a scoop and returned to the reservoir. A stainless-steel diatomite spin filter is used to remove foreign particles from the water reservoir and hence prevent nozzle clogging and erratic flow control.

The water system is able to deliver 340 gallons of water per minute, creating a water layer 12-in. wide and 0.1-in. thick, flowing at a speed of 90 feet per second.

(b) Nozzle

Figure 3 is a closeup view of the nozzle. The first section of the nozzle is a transient device which connects the 3-in.-diam circular pipe to the rectangularly shaped inlet of the second nozzle section, the thickness-adjusting box. The transient section is 28-3/4 inches in length; it has an inside diameter of 3 inches on one end and at the other a rectangular cross-section 12-in. long and 0.50-in. wide. The thickness-adjusting box contains a metal plate hinged at one end and free at the other. The distance between the

free end of the plate and the bottom part of the nozzle is adjusted by inserting rods of various thickness between the hinged plate and the top of the thickness-adjusting box. There is a groove on the top face of the hinged plate to accommodate these rods. Since standard rods are available in increments of 0.01 inches, almost any desired opening within the limits of the nozzle (approximately 0.5 inch) may be obtained. Under normal operating conditions the water pressure within the adjusting box is more than sufficient to keep the hinged plate from falling (at 150-ft head, the force is near 5,000 lb); however, two thumb screws are provided to pull the plate firmly against the rod.

The bottom (non-movable) plate of the thickness-adjusting box is aligned to be tangent with the test section of the rolling road so that the water jet and road meet smoothly.

Tire Rig

The test tires are mounted on a nose-wheel assembly from a Grumman MOHAWK aircraft modified to accommodate tires up to 12 inches in diameter and 7 inches in width, and to allow for instrumentation. Figures 6 and 7 show, respectively, front and back views of the tire rig.

The upper part of the strut which guides the wheel cylinder is fixed to a structure above the rolling road. This structure can be located anywhere along the rolling road. The wheel fork and its cylinder are free to heave (move vertically). To provide minimum heave friction, a lubricated brass sleeve is inserted between the male and female members of the vertical strut. During operation this sleeve is rotated by a 1/4-hp motor. The effect is to provide lubricated dynamic friction rather than static friction between the members. The entire movable section is counterbalanced by an appropriate counterweight.

A shaft capable of accommodating tires of various sizes is mounted at the end of the fork. The wheel is installed parallel to the longitudinal axis of the rolling road and is not free to move laterally. The rotation of the wheel shaft is transmitted through a timing belt to an upper shaft in which an electric brake is mounted. A symmetrical loading platform is installed on the fork.

The entire tire rig is mounted on bearings which allow the rig freedom to swing, pendulum fashion, along the longitudinal axis of the road. Restricting this motion, however, is a parallelogram linkage system connected to a force transducer (see discussion under "Instrumentation").

Instrumentation

(a) Horizontal (Longitudinal) Force Exerted on the Tire (H)

A spring beam, fixed at one end, restrains the parallelogram linkage of the tire rig. Connected to this spring beam is a linear variable differential transformer which measures the deflection of the beam and, correspondingly, the longitudinal force on the tire rig (the measurement signal is electronically recorded on paper tape). This device is accurate to within ± 0.1 lb.

(b) Tire Load (W)

Tire load is maintained constant by counterbalancing the weight on the tire and then placing known weights on the load platform. When the sleeve insert is rotating, vertical friction is less than 0.3 lb.

(c) Linear Road Speed (V)

Linear road speed is measured by a tachometer-generator attached to the idler pulley of the rolling road. Tach output is recorded on paper tape. Water velocity, which must match belt speed, is presently computed by dividing the volume flow, as measured in the nozzle entrance pipe, by the exit area of the nozzle. The accuracy of this method is still to be proved; however, no alternative techniques which are satisfactory have yet been found.

(d) Tire Rotational Speed (ω)

A tachometer-generator is attached to the upper shaft of the tire rig. A timing belt ensures turning of upper shaft and tire at the same speed.

(e) Fluid Viscosity (μ), Density (ρ) and Surface Tension (σ)

These are obtained from standard tables after water-temperature measurements.

(f) Upstream Fluid Depth (h)

A modified micrometer, attached so that it can be positioned both longitudinally and laterally across the belt, is installed above the rolling road. A feeler attached to the micrometer is able to measure surface-height differences. This device has not proved entirely satisfactory, since there is a small hop in the belt and there are some surface waves on the water. Improved measurement techniques are being investigated. Correlation of water height with nozzle opening has not yet been established.

(g) Tire Diameter (D)

In all cases this represents the undeflected dimension at the point of maximum diameter.

(h) Tire-Road Friction (f)

This is computed as the ratio of the measured horizontal force exerted on a fully braked (locked) tire, when the road is moving at a constant slow speed, to the imposed load.

STATIC TESTS OF MODEL TIRES

One of the prime requisites for the conduct of the hydroplaning model-test program planned here is a selection of model tires of systematically varying dimensions, whose mechanical properties simulate accurately those of representative aircraft tires. It was discovered at an early stage that the available selection of commercial pneumatic tires under 12 inches in diameter is extremely limited, and that the cost of fabricating such tires to specifications would be prohibitive. Semi-pneumatic tires were available in much greater variety in the sizes of interest; but these, not unexpectedly, were found to possess mechanical properties very dissimilar to those desired.

Earlier studies conducted at the Davidson Laboratory[3,4] had demonstrated that a tire fabricated of solid polyurethane foam performs, in many respects, like an inflated pneumatic tire. By changing the density of the foam (controlled by the mix used in manufacturing), different tire pressures may be simulated. Also, the size and tightness of metal side plates can be varied to simulate the effects of sidewall stiffness. By careful machining on a lathe, a polyurethane cylinder can be given a reasonable tire contour. Absorption of water by the (open cell) polyurethane foam can be controlled by the application of a plastic waterproof coating without materially altering deformation characteristics.

To explore further the feasibility of simulating pneumatic aircraft tires with polyurethane-foam models, a series of preliminary tests was conducted with models fabricated of foams of various densities (between 13 lb/ft^3 and 16 lb/ft^3), plus a single small industrial pneumatic tire for comparison. Measurements taken of static load-deformation characteristics (see below) were compared with various empirical formulas shown by Smiley and Horne to describe the properties of modern pneumatic aircraft tires.[9] Some dynamic tests were also conducted, but no quantitative data were taken. Qualitatively, however, the urethane tires appeared in all respects to behave very similarly to the pneumatic control tire.

Test Procedure

Experiments were conducted with the tires shown in the following table.

Size (Diam x Width)	Description
6" x 2"	Polyurethane foam; density 15.9 lb/ft^3; Type I profile*
6" x 2"	Polyurethane foam; density 15.2 lb/ft^3 (estimated**); elliptic profile
6" x 2"	Polyurethane foam; density 14.6 lb/ft^3; Type III profile*
6" x 2"	Polyurethane foam; density 13.0 lb/ft^3; elliptic profile
8.5" x 3"	Industrial pneumatic 280/250-4 (see Ref. 10)

The tests were conducted with the tire rig shown in Figure 8. The tire was loaded vertically by placing weights on a loading platform over the axle. To eliminate possible irregularities around the tire, four points 90-degrees apart were tested and measurements at these four points were averaged for every vertical load.

For footprint geometry measurements, the tire surfaces were coated with black ink. The painted surface of the tire was then rested on a white sheet of paper so as to produce an ink impression of the footprint area. From these prints the over-all length (ℓ) and width (b) of the footprint were measured. The surface area (A) of the footprint was measured with a planimeter. Vertical tire deflection (δ) was measured with a mechanic's height gage (shown in Figure 8).

The pneumatic tire was tested with three different inflation pressures: 15, 32, and 55 psi. Polyurethane tires were tested both with 4- and 5-in.-diam aluminum side plates and without side plates.

---

*Aircraft tires are type-classified according to general appearance and profile geometry. Type definitions may be found in Reference 9.

**This tire was accidentally destroyed before weight/volume measurements were taken and its density therefore had to be estimated from the results.

Test Results

Vertical-Force-Deflection Variations. – Figure 9 is a plot of the vertical-force-deflection measurements for each of the polyurethane model tires tested with 4-in.-diam side plates. The curves all have the same general form and, as might be expected, the resistance to deformation increases uniformly with increasing foam density. This indicates qualitatively how the effect of pneumatic-tire inflation pressure may be simulated with the foam-model tires. The effect of side-plate diameter on the foam-tire deflection characteristics is shown in Figure 10. Qualitatively again, the similarity to the effect of pneumatic-tire carcass stiffness is apparent.

The quantitative relationship between the load-deflection properties of the polyurethane foam tires and modern pneumatic aircraft tires was investigated on the basis of the following empirical formulas developed by Smiley and Horne.[9]

$$\frac{W}{(P + 0.08P_r)w\sqrt{wD}} = 0.96(\delta/w) + \frac{0.216(\delta/w)^2}{C_z} \quad \left(\text{For: } \delta/w \leq \frac{10}{3} C_z\right)$$

$$\frac{W}{(P + 0.08P_r)w\sqrt{wD}} = 2.4\left[(\delta/w) - C_z\right] \quad \left(\text{For: } \delta/w \geq \frac{10}{3} C_z\right) \tag{15}$$

where

P_t	$(P + 0.08P_r)$ total pressure
P	inflation pressure of tire
P_r	rated pressure of tire
C_z	0.02 for Type I aircraft tires 0.03 for Types III and VII aircraft tires
W	vertical load on tire
δ	vertical deflection
D	outside diameter of free tire
w	maximum width of undeflected tire

The data of Figures 9 and 10 were fitted to the following modified form of Equations (15).

$$\frac{W}{P_{eq}\, w\sqrt{wD}} = 0.96\ (\delta/w) + \frac{0.216(\delta/w)^2}{C_z} \quad \left(\text{For: } \delta/w \le \frac{10}{3} C_z\right)$$

$$\frac{W}{P_{eq}\, w\sqrt{wD}} = 2.4\left[(\delta/w) - C_z\right] \quad \left(\text{For: } \delta/w \ge \frac{10}{3} C_z\right) \tag{16}$$

where P_{eq}, the "equivalent total pressure" of a polyurethane foam tire, is a function of both foam density and side-plate diameter.

The P_{eq} values derived in this manner for each tire, given in the table below, were then used to compute the values of the vertical-force parameter $\frac{W}{P_{eq}\, w\sqrt{wD}}$ plotted in Figures 11 and 12 along with the corresponding curves derived from Equation (16).*

EQUIVALENT TOTAL PRESSURE OF POLYURETHANE-FOAM MODEL TIRES

Type	Foam Density (lb/ft^3)	Side Plate diam (in.)	P_{eq} (psi)
I	15.9	4	23.5
Elliptic	15.2	5	19.8
Elliptic	15.2	4	18.2
Elliptic	15.2	0	18.2
III	14.6	4	12.1
Elliptic	13.0	4	6.6
Elliptic	13.0	0	5.6

These graphs show that the measured data are in excellent agreement with the fitting equation. In fact, the degree of scatter from the curves appears

*The value of C_z for elliptic profile tires was determined from the data analysis to be equal to 0.02 (the same as for the Type I tires).

to be even less than that exhibited by the aircraft-tire data from which Equations (15) were originally derived. Thus it may be concluded that the static vertical-load-deflection characteristics of the polyurethane tires are indeed similar to those of the modern pneumatic aircraft tire, and that the "equivalent total pressure" of one of the foam tires represents the total pressure of a pneumatic aircraft tire of the same geometry and with the same vertical-load-deflection characteristics.

Insufficient data are available at this time to establish precisely the general quantitative relationship of pneumatic-tire inflation and carcass pressures to foam-tire density and side-plate diameter. An indication of the general nature of such a relationship, however, may be seen in Figure 13, which is a plot of equivalent total pressure vs. foam density for each of the polyurethane tires tested with 4-in.-diam side plates.

Geometric Properties of Footprint Area. — Measured geometric footprint properties of each of the aircraft-profile polyurethane tires, with 4-in.-diam side plates, are shown in graphical form in Figure 14. Plots are given of the footprint-length parameter, ℓ/D, vs. the vertical-deflection parameter, δ/D; and of the footprint-width parameter, b/w, and footprint-area parameter, $A/w\sqrt{wD}$, vs. the vertical-deflection parameter, δ/w. Plotted on the same graphs are lines corresponding to the equations below, shown by Smiley and Horne to describe the geometric footprint properties of representative pneumatic aircraft tires under pure vertical loading.[9]

$$\ell/D = 1.7\sqrt{(\delta/D) - (\delta/D)^2} \tag{17}$$

$$b/w = 1.7\sqrt{(\delta/w) - 2.5(\delta/w)^4 + 1.5(\delta/w)^6} \tag{18}$$

$$A = 2.3\,\delta\sqrt{wD} \tag{19}$$

where ℓ = length of tire-ground contact area (footprint)

b = width of tire-ground contact area (footprint)

A = gross footprint area

and the other symbols are as defined earlier.

The graphs of Figure 14 show that the measured geometric footprint properties of the polyurethane tires agree quite well with the relations derived from data for the full-scale pneumatic aircraft tire.

CONCLUDING REMARKS

A laboratory setup has been developed for the conduct of scale-model experiments to investigate the tire-hydroplaning phenomenon. Model tires fabricated of polyurethane foam have been shown to exhibit static load-deflection characteristics which accurately simulate the properties of full-scale pneumatic aircraft tires. It is felt that the logical next step in the program is the verification of the basic experimental approach on the basis of comparisons of actual test data with appropriate full-scale results generated previously at NASA Langley. To this end, an initial test program has been formulated to measure hydroplaning inception speed (V_{cr}) as a function of tire-loading and tire-geometry.

The experiment will consist of an investigation of the effects of each of the independent variables h/D, w/D, and δ/D on the "critical dynamic hydroplaning parameter" $\rho D^2 (V_{cr})^2/W$, for a systematic series of model tires with rectangular cross-section and no tread. Figure 15 illustrates the experimental design in terms of a sample data sheet.

The experimental results will be compared with the data for full-scale pneumatic aircraft tires presented by Horne and Joyner,[2] and will also be analyzed to determine Froude number, Reynolds number, and Weber number effects (see discussions under "Analysis"). On the basis of these investigations, general conclusions will be drawn regarding the validity of the experimental approach, and recommendations will be made for the future course of work under this program.

Davidson Laboratory,
Stevens Institute of Technology
Hoboken, N. J., August 29, 1967.

REFERENCES

1. Horne, W. B.; and Dreher, R. C.: Phenomena of Pneumatic Tire Hydroplaning. NASA TN D-2056, 1963.

2. Horne, W. B.; and Joyner, U. T.: Pneumatic Tire Hydroplaning and Some Effects on Vehicle Performance. Society of Automotive Engineers, 970C, January 1965.

3. Dugoff, H., et al: Coupled Mobility Devices. Davidson Laboratory Report 1164, Stevens Institute of Technology, December 1964.

4. Jurkat, M. J.; and Starrett, J. A.: Automobile-Barrier Impact Studies Using Scale Model Vehicles. Highway Research Record No. 174, HRB Publication 1505, 1967.

5. Dugoff, H.: "The Davidson Laboratory Rolling Road Facility." Journal of Terramechanics, Vol. 1, No. 4, 1964.

6. Soper, W. G.: "Scale Modeling." International Science and Technology, No. 62, February 1967.

7. Murphy, G.: Similitude in Engineering. Ronald Press, New York, 1950.

8. Todd, F. H.: The Fundamentals of Ship Model Testing. Society of Naval Architects and Marine Engineers, 1951.

9. Smiley, R. F.; and Horne, W. B.: Mechanical Properties of Pneumatic Tires with Special Reference to Modern Aircraft Tires. NASA TR R-64, 1960.

10. Tire and Rim Association Year Book, 1963.

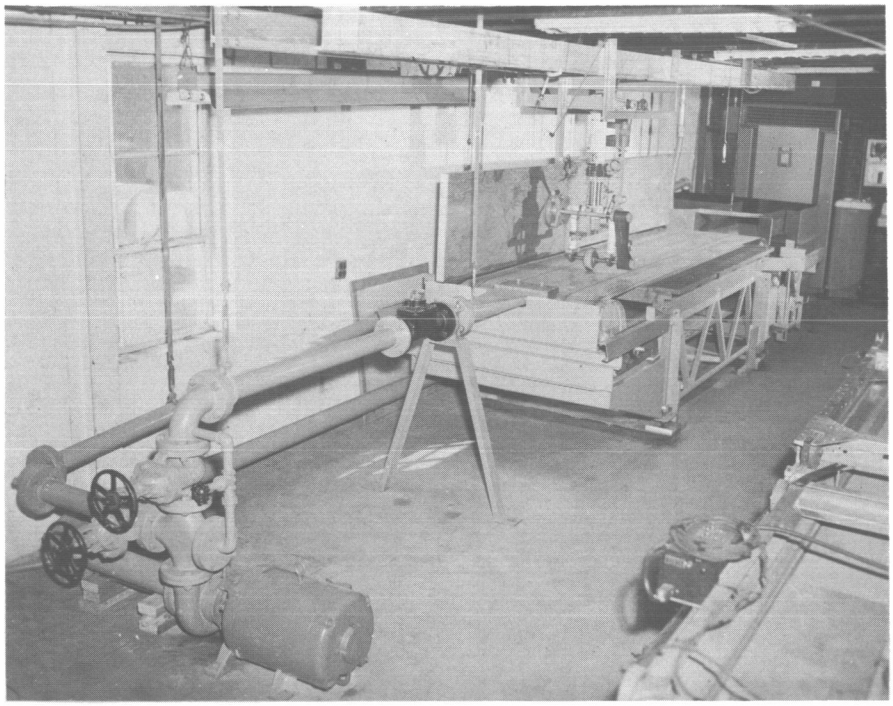

Figure 1. General View of the Davidson Laboratory Tire-Hydroplaning Test Facility

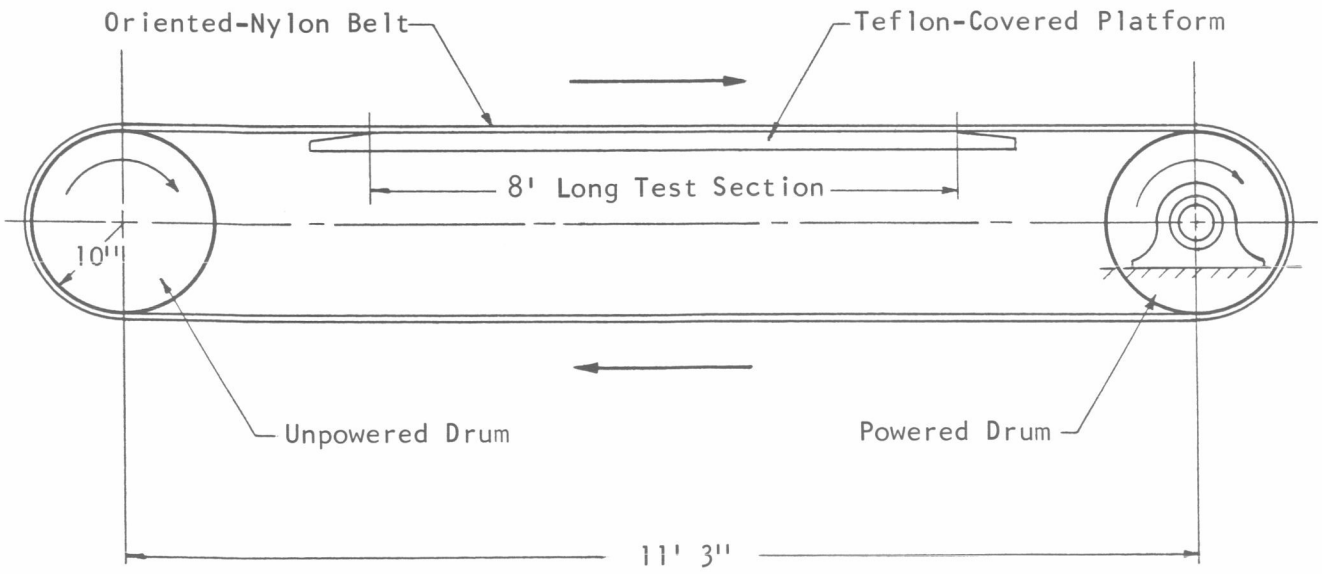

Figure 2. Schematic Illustrating Operation of Rolling Road

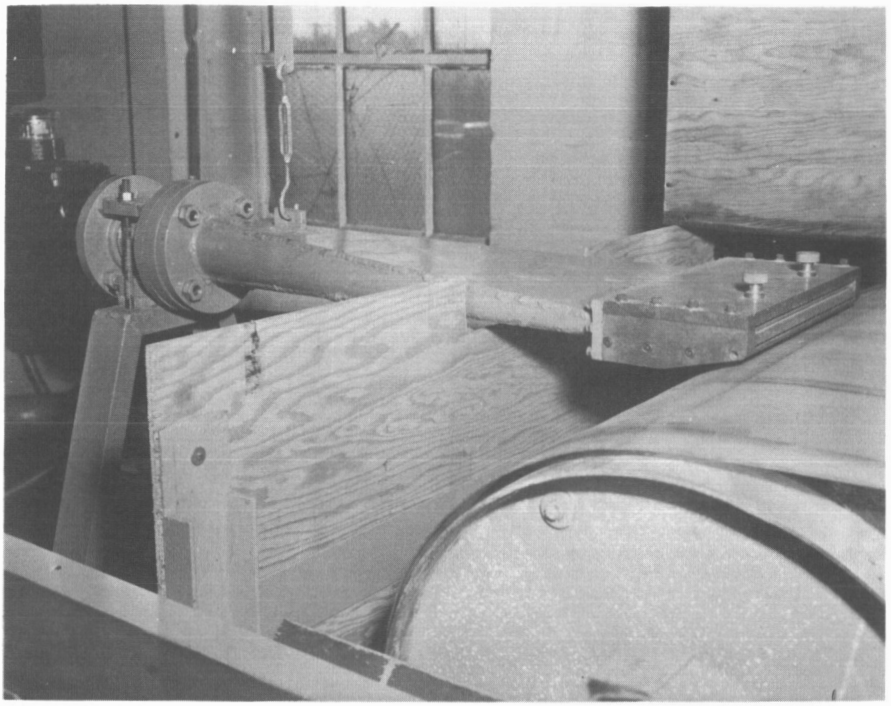

Figure 3. Close-up View of Water-Supply Nozzle

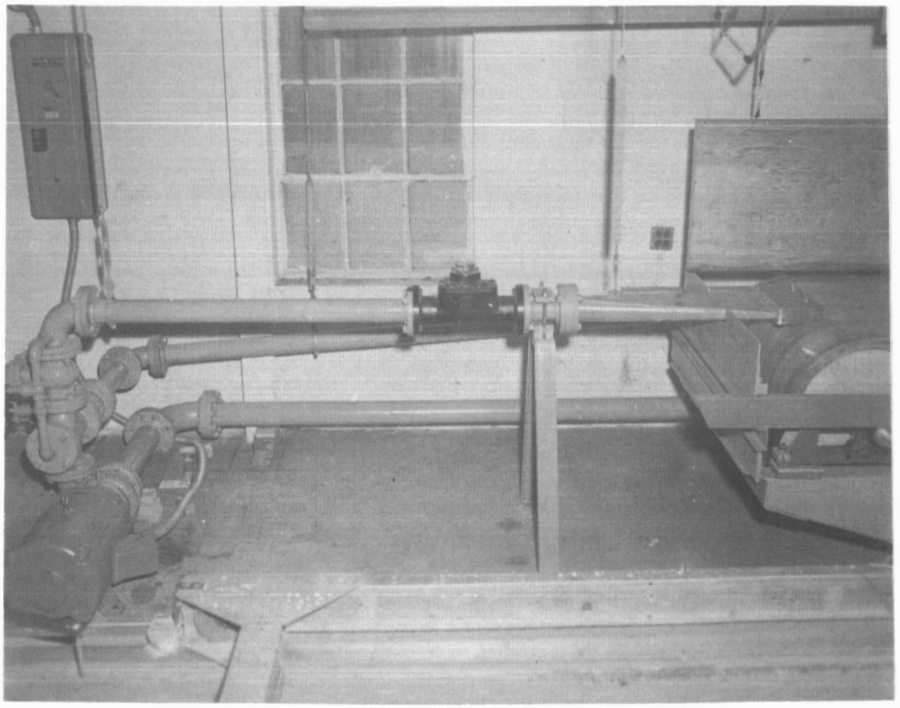

Figure 4. Over-all View of Water-Supply System

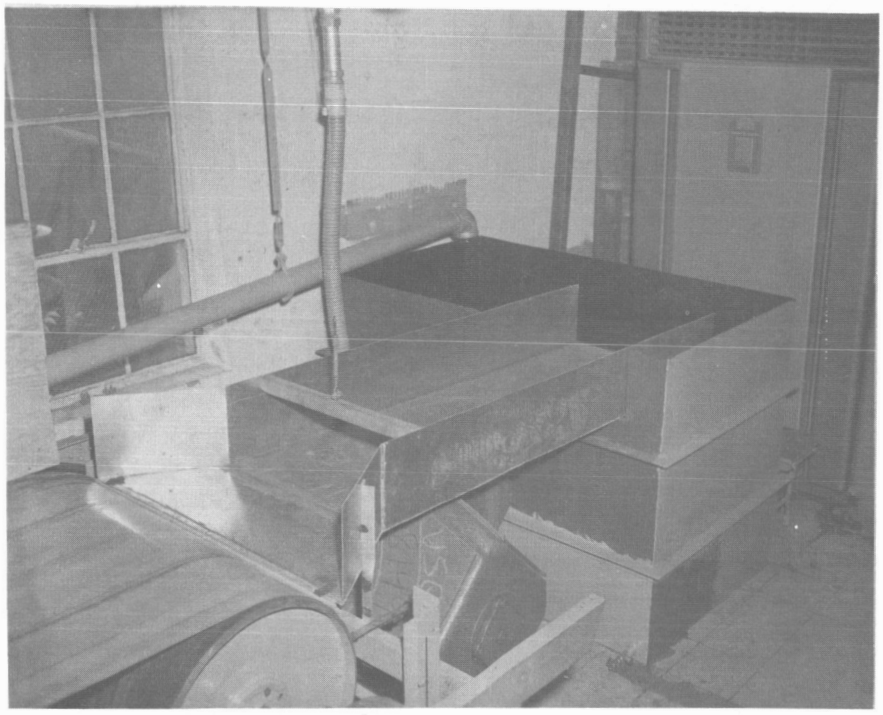

Figure 5. Water-Return Scoop, Reservoir, and Piping

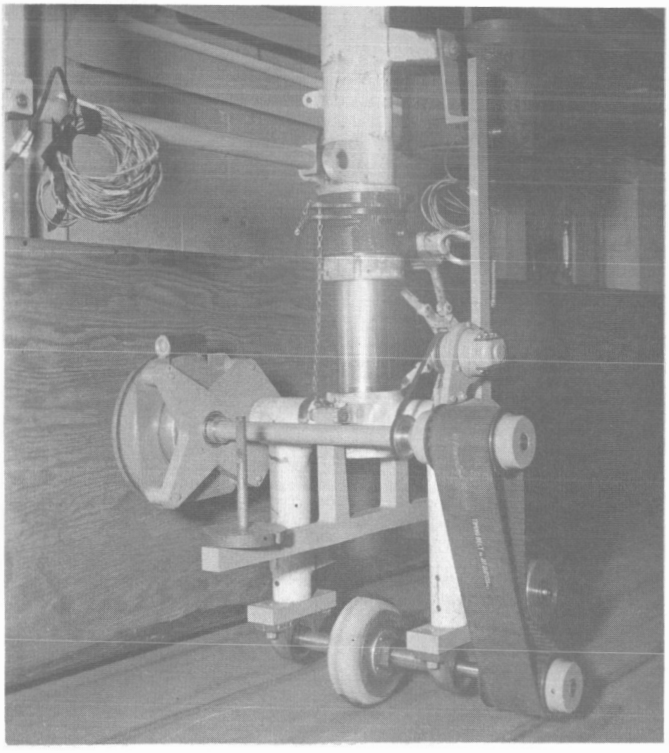

Figure 6. Front View of Tire Test Rig With Polyurethane Model Tire

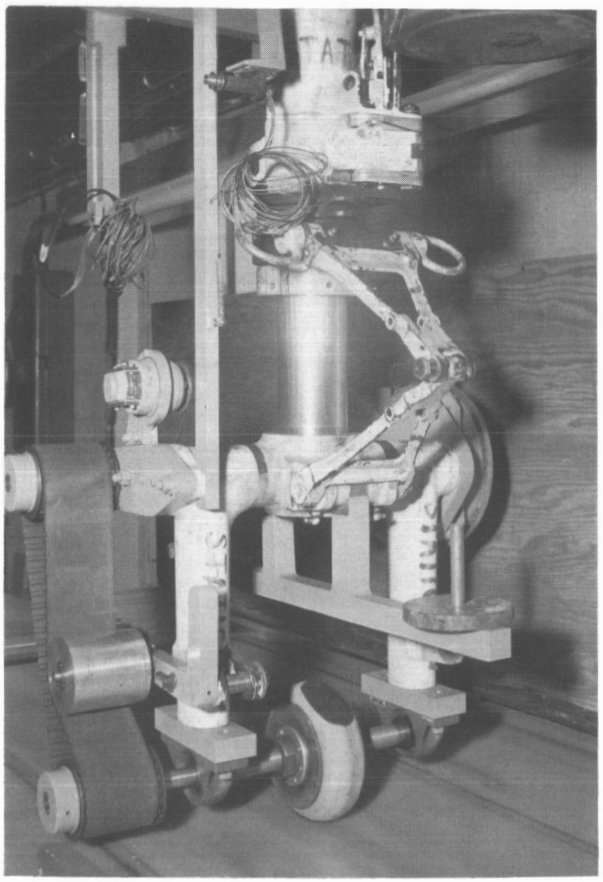

Figure 7. Rear View of Tire Test Rig With Polyurethane Model Tire

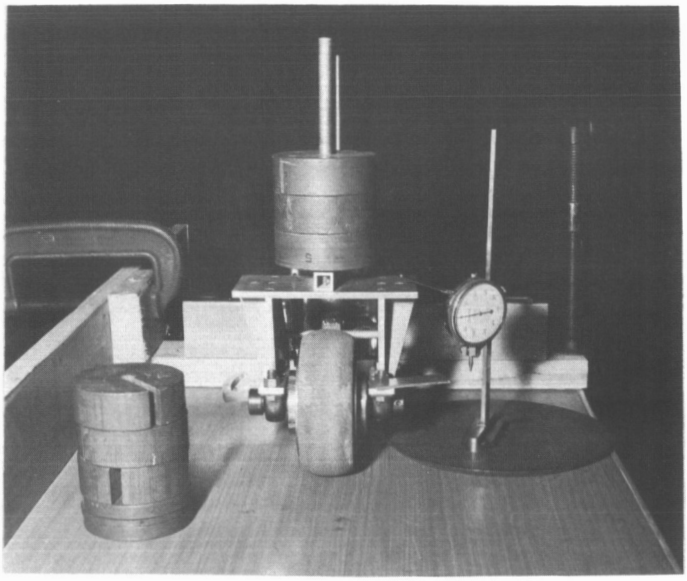

Figure 8. Static Tire-Test Setup

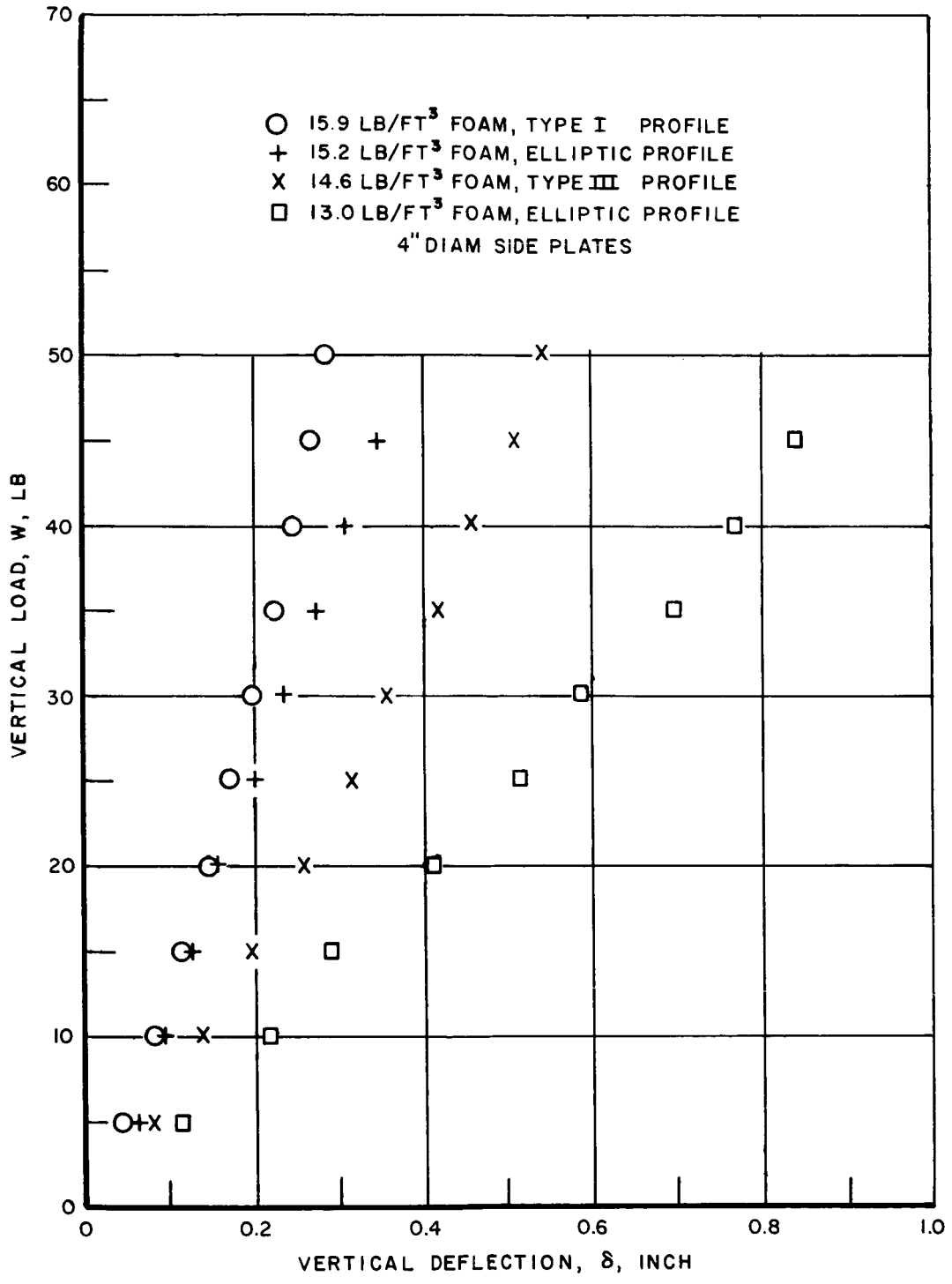

FIGURE 9. VERTICAL-LOAD-DEFLECTION VARIATION FOR POLYURETHANE TIRES WITH 4" DIAMETER SIDE PLATES, VARIOUS FOAM DENSITIES AND PROFILES

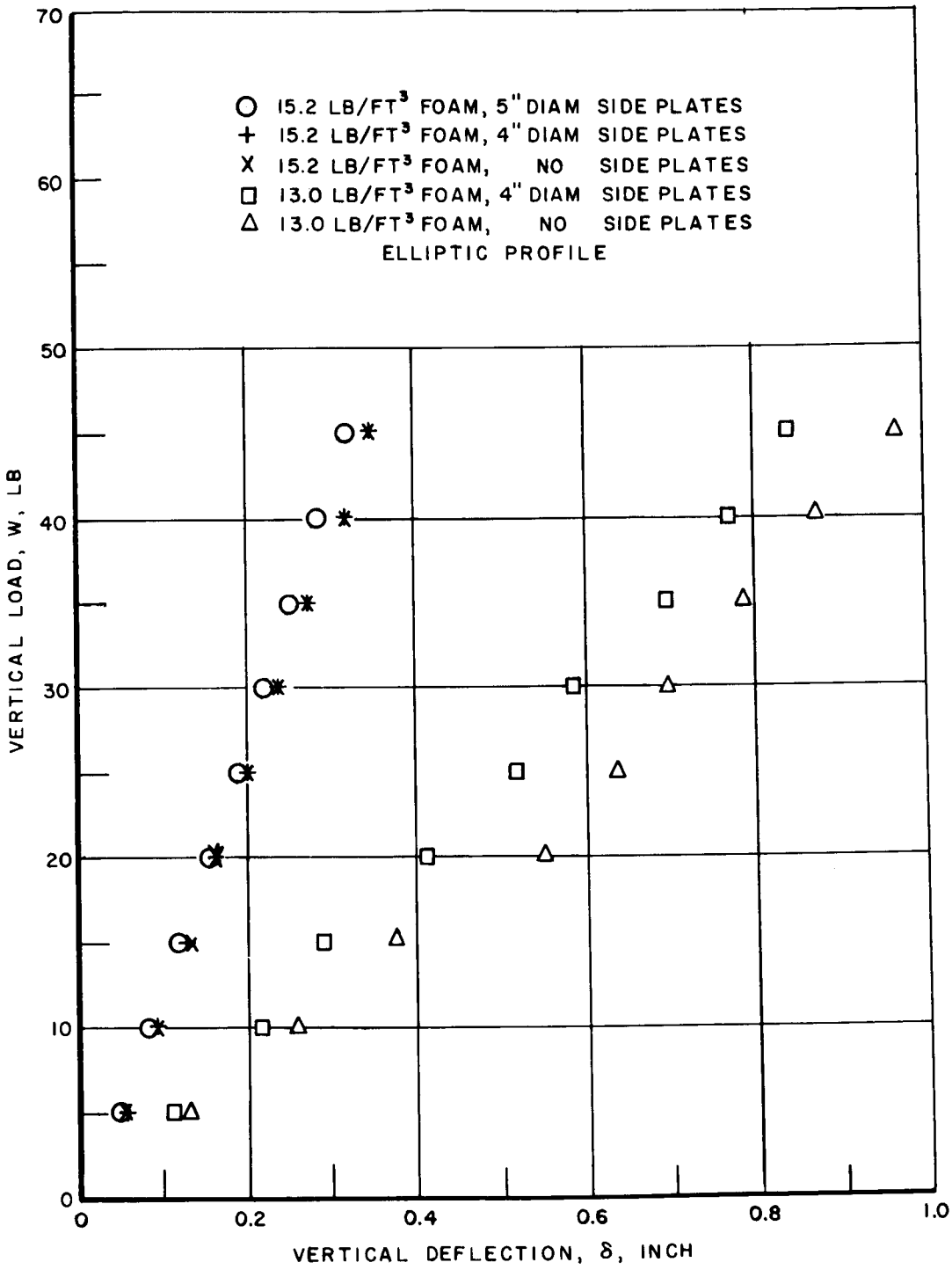

FIGURE 10. EFFECT OF SIDE-PLATE DIAMETER ON VERTICAL-LOAD-DEFLECTION VARIATION OF POLYURETHANE TIRES

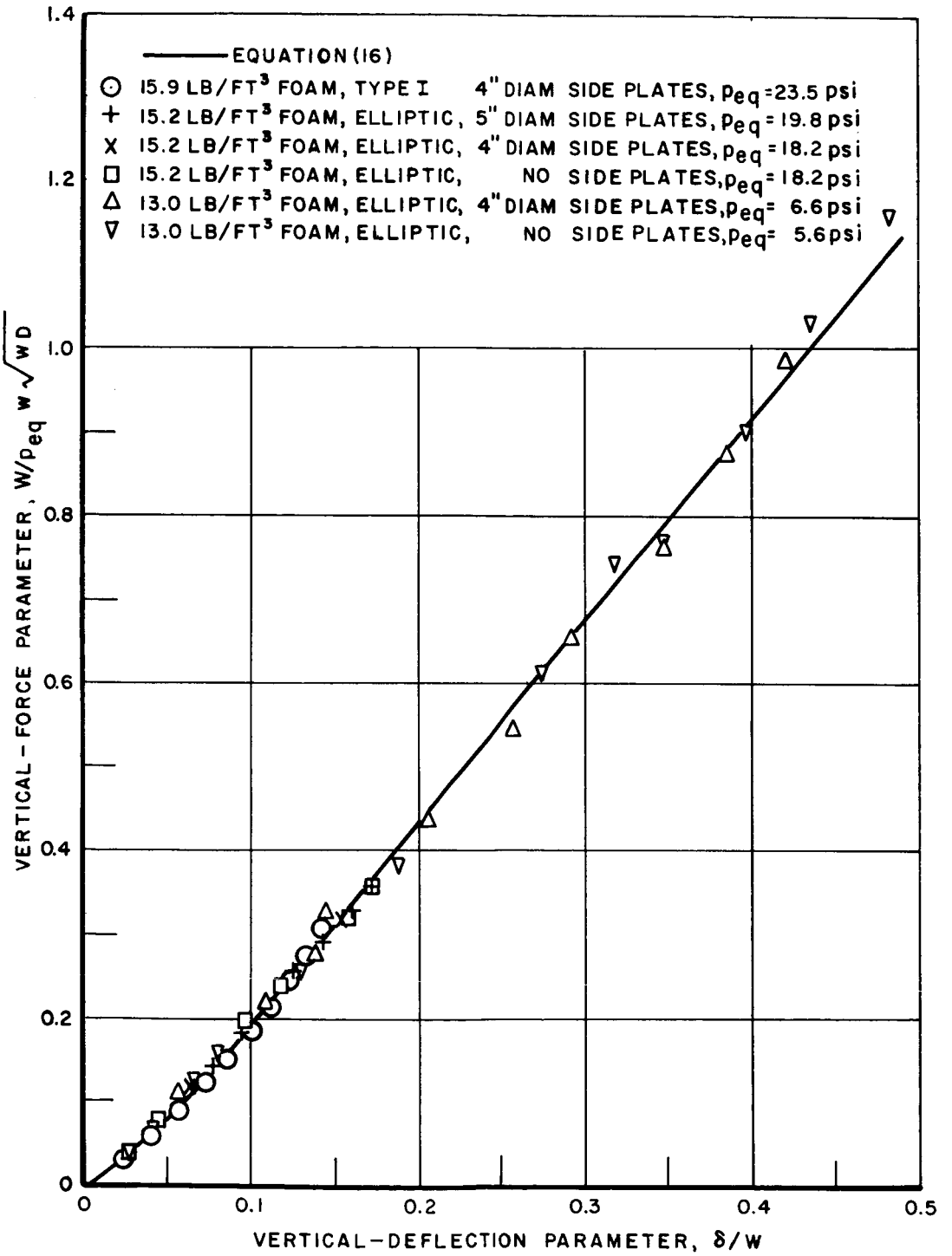

FIGURE 11. VARIATION OF VERTICAL-FORCE PARAMETER WITH VERTICAL DEFLECTION PARAMETER FOR TYPE I AND ELLIPTIC-PROFILE POLYURETHANE MODEL TIRES

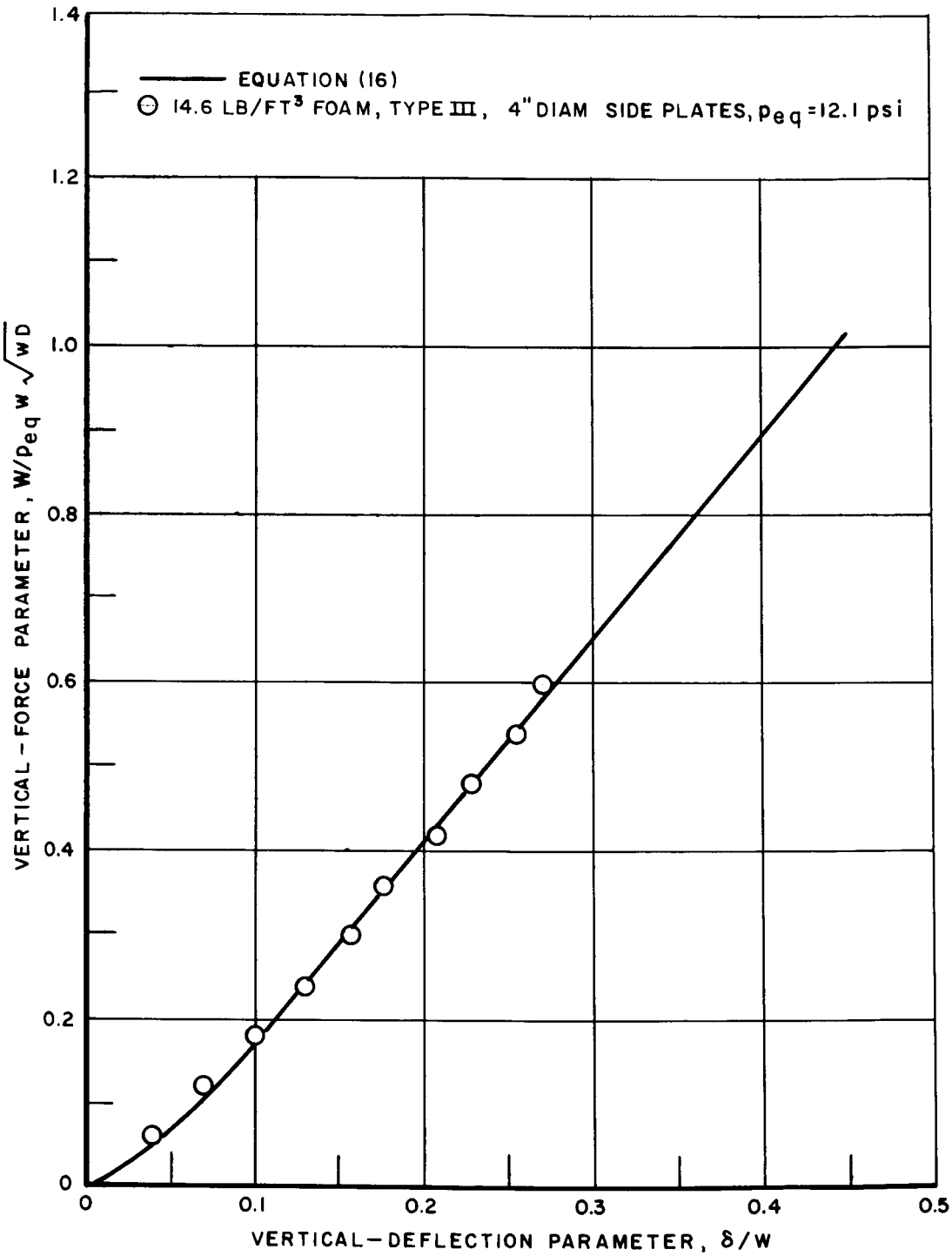

FIGURE 12. VARIATION OF VERTICAL-FORCE PARAMETER WITH VERTICAL DEFLECTION PARAMETER FOR TYPE III POLYURETHANE MODEL TIRE

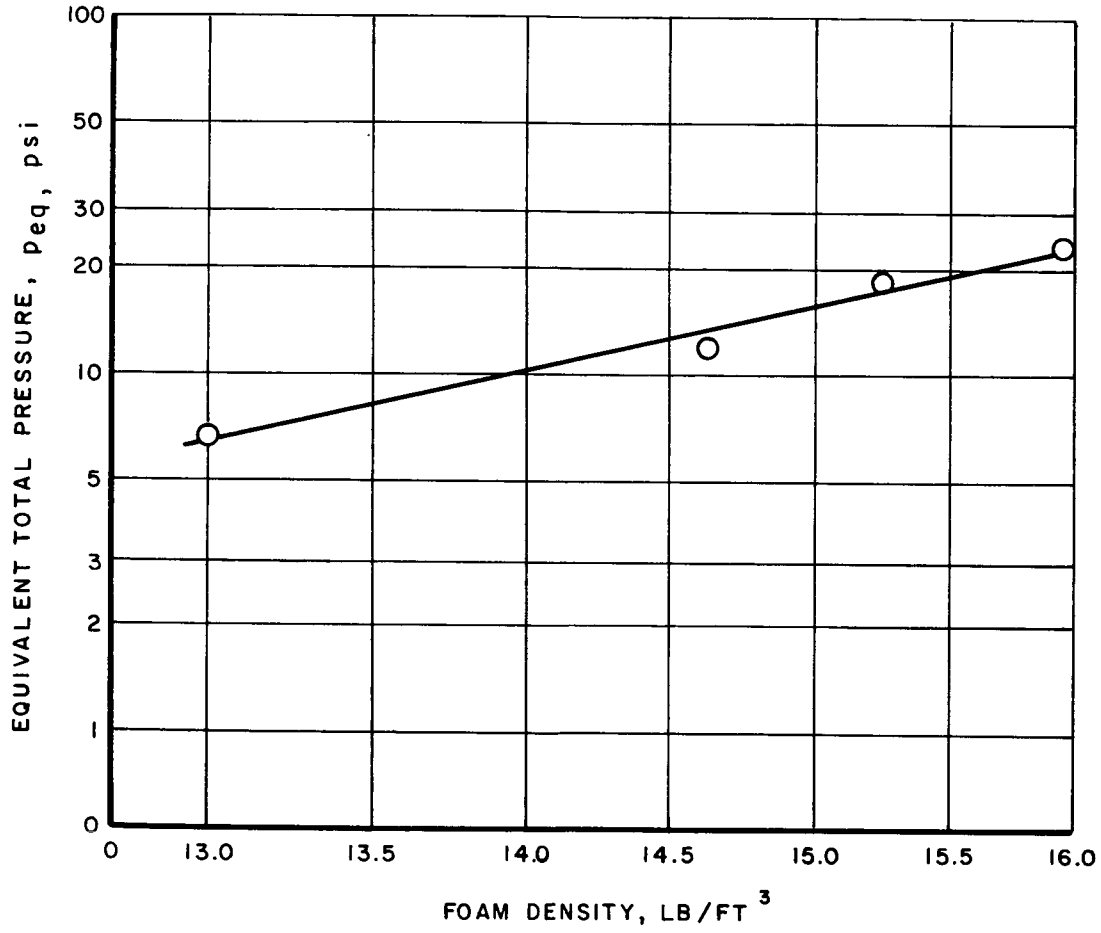

FIGURE 13. VARIATION OF EQUIVALENT TOTAL PRESSURE WITH FOAM DENSITY FOR POLYURETHANE TIRES WITH 4" DIAMETER SIDE PLATES

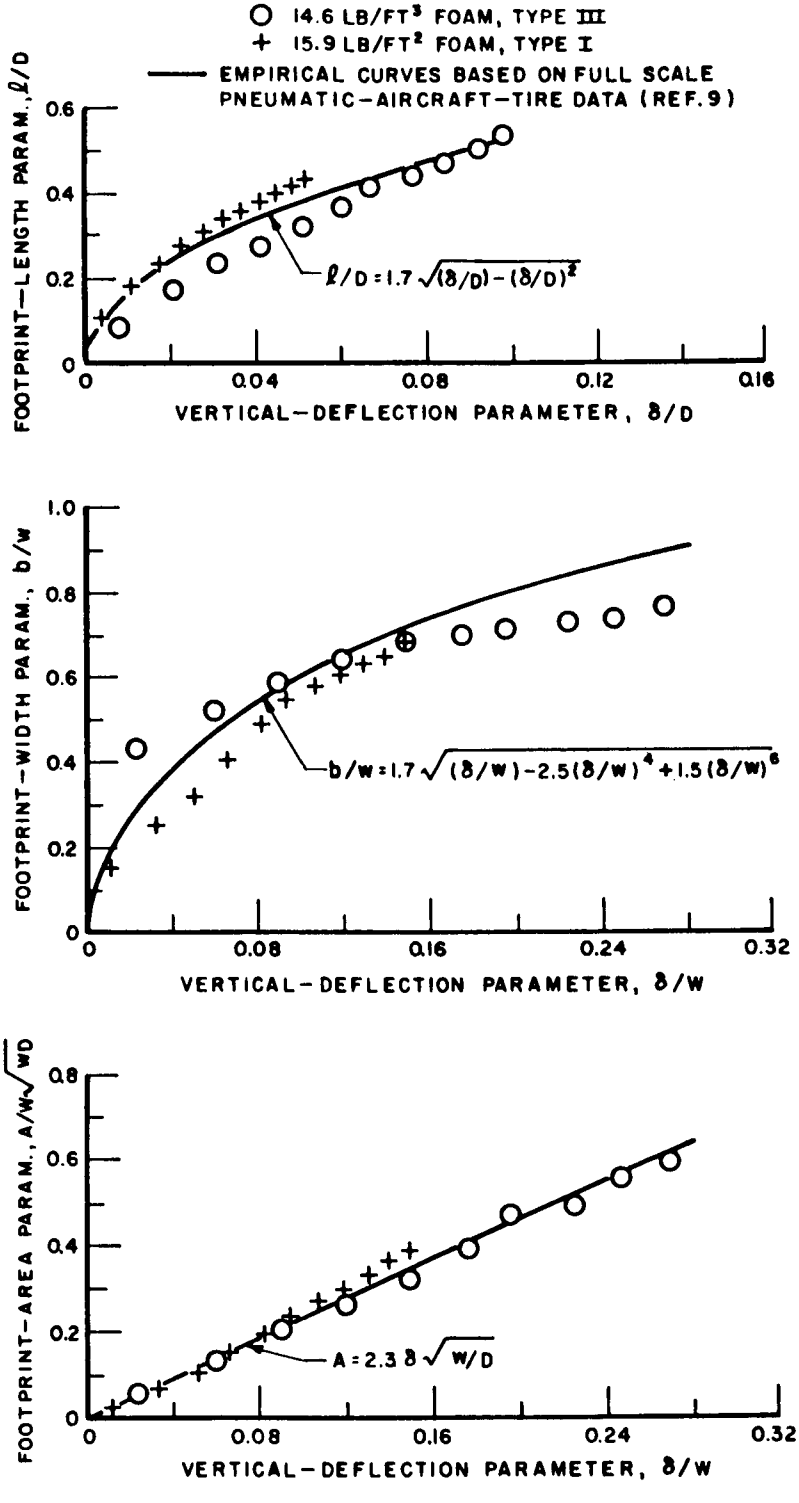

FIGURE 14. GEOMETRIC PROPERTIES OF FOOTPRINT AREA, POLYURETHANE MODEL TIRE WITH 4" DIAMETER SIDE PLATES

W	δ/D	w	w/D	h_1/D	V_{cr}	h_2/D	V_{cr}	h_3/D	V_{cr}	h_4/D	V_{cr}
W	δ_1/D										
W	δ_2/D		0.668								
W	δ_3/D										
W	δ_1/D										
W	δ_2/D		0.400	CONSTANT		CONSTANT		CONSTANT		CONSTANT	
W	δ_3/D										
W	δ_1/D										
W	δ_2/D		0.285								
W	δ_3/D										
W	δ_1/D										
W	δ_2/D		0.222								
W	δ_3/D										

Figure 15. Sample Data Sheet for Initial Test Program